Quantum-Impurity Relaxometry of Magnetization Dynamics

B. Flebus and Y. Tserkovnyak
Department of Physics and Astronomy, University of California, Los Angeles, California 90095, USA

(Received 6 April 2018; revised manuscript received 19 July 2018; published 2 November 2018)

Prototypes of quantum impurities, such as NV and SiV color centers in diamond, have garnered much attention due to their minimally invasive and high-resolution magnetic field and thermal sensing. Here, we investigate quantum-impurity relaxometry as a method for probing collective excitations in magnetic insulators. We develop a general framework to relate the measurable quantum-impurity relaxation rates to the intrinsic dynamic properties of a magnetic system via the noise emitted by the latter. We suggest, in particular, that the quantum-impurity relaxometry is sensitive to dynamic phase transitions, such as magnon condensation, and can be deployed to detect signatures of the associated coherent spin dynamics, both in ferromagnetic and antiferromagnetic systems. Finally, we discuss prospects to nonintrusively probe spin-transport regimes and measure the associated transport coefficients in magnetic insulators.

DOI: 10.1103/PhysRevLett.121.187204

Introduction.—Quantum impurities (QIs), such as NV and SiV centers in diamond, display an exceptional sensitivity to static magnetic fields and their spin state can be initialized and read out optically [1–5]. These defects can noninvasively resolve magnetic textures on length scales of the order of tens of nanometers, without requiring strong external polarizing fields [6]. Their relaxation rates are, furthermore, affected by the electromagnetic noise in its vicinity, encapsulating information about the dynamic properties of the environment. In equilibrium, this is rooted in the fluctuation-dissipation theorem [7], which relates the noise to the physical response function.

While QI relaxometry has already been proposed as a platform for studying transport properties and spatial inhomogeneities in electronic systems [8], an analogous theoretical framework for magnetic insulators is still in its infancy. The QI ability to probe noise locally and nonintrusively, however, appears particularly appealing for magnetic insulating systems [9], as the detection of their collective excitations, such as spin waves, is, otherwise, largely limited to conventional spin-transport experiments [10,11] or microwave probes [12]. As we discuss below, the QI relaxometry may offer a number of clear advantages, such as a direct bulk measurement of spin-transport coefficients.

Heretofore, spin-wave relaxometry has been focusing only on the noise emitted by a magnetic system at frequencies higher than its spin-wave gap [6,9,13]. For a ferromagnet, this noise reflects both the spectrum and the distribution of its magnon gas at the QI resonance frequency [9]. Following this approach, Du *et al.* [9] have provided the first direct measurement of the magnon chemical potential, as well as its dependence on external perturbations, in a ferromagnetic system. However, a variety of magnetic systems possess spin-wave gaps that are much larger than the maximum operating frequency of, e.g., NV centers [6]. In particular, the relaxometry of antiferromagnetic insulators, which have been attracting much attention lately owing to their ultrafast spin dynamics [14], has not yet been undertaken due to the lack of a theoretical framework for the magnetic subgap noise. In this Letter, therefore, we address the detection, via QI relaxometry, of the magnetic noise emerging at subgap frequencies.

The interaction between spin waves and a QI spin induces transitions between its quantum states. When the spin relaxes, it releases an energy proportional to its resonance frequency, as shown in Fig. 1(a). How this

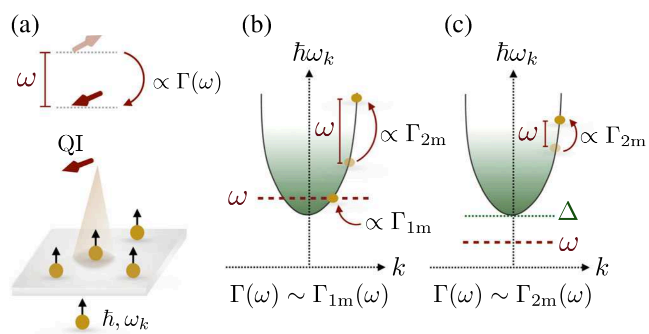

FIG. 1. Quantum-impurity relaxation via one- and two-magnon processes. (a) The interaction between the QI spin and a nearby magnetic system, here, depicted as gas of magnons with spin $\hbar$ and frequency ω_k (with $\omega_{k=0} = \Delta$), leads to a QI transition with emission of energy $\hbar\omega$. (b) When $\omega > \Delta$, the latter can result in the creation of a magnon at frequency $\omega_k = \omega$ or in a magnon (Raman) scattering with energy gain $\hbar\omega$. These events contribute, respectively, to the single-magnon, $\Gamma_{1\,m}$, and two-magnon, $\Gamma_{2\,m}$, QI relaxation rates. When $\omega > \Delta$, the relaxation rate is typically dominated by the one-magnon processes. (c) Conversely, for $\omega < \Delta$, one-magnon events are suppressed and $\Gamma \approx \Gamma_{2\,m}$. Similar processes, in reverse, are responsible for the QI transitions with absorption of energy $\hbar\omega$.

energy is converted into excitations of the magnetic system depends on the gap of the spin-wave spectrum. If the QI resonance frequency is larger than the spin-wave gap, the relaxation can trigger both one- and two-magnon processes, corresponding, respectively, to the creation of a magnon at the QI resonance frequency or to a magnon scattering with energy gain equal to it, as depicted in Fig. 1(b). One can show, by using a simple model of a local coupling between the QI spin and the ferromagnetic spin density of an ideal magnon gas, that the relaxation rate, Γ_{2m}, due to the two-magnon processes is suppressed at low temperatures with respect to the one-magnon, Γ_{1m}, one: $\Gamma_{1m} \sim T/T_C$ while $\Gamma_{2m} \sim (T/T_C)^2$, in terms of the Curie temperature T_C. When the QI resonance frequency lies within the gap, however, the one-magnon scattering is prohibited and two-magnon processes overtake the QI transitions, as shown in Fig. 1(c). Focusing on this regime, we develop a theory of relaxometry driven by two-magnon noise.

To illustrate its capability of probing spin-transport properties and detecting dynamic phase transitions, we discuss two main examples. First, we focus on the characterization of a diffusive spin-wave transport, which is relevant in the context of magnetic insulator-based devices. Heretofore, these properties have been investigated in metallic-insulating heterostructures, where invasive metallic contacts are used for spin injection and detection [10,11]. In such setups, the spin interconversion at the metal-insulator interface depends on a variety of parameters and length scales, which might hinder the extraction of a bulk signal. Here, we show how the QI relaxometry driven by two-magnon noise can overcome these drawbacks, allowing us to probe the intrinsic bulk spin-transport properties directly. Finally, we investigate the dependence of the two-magnon noise on the spin chemical potential in both ferromagnetic and antiferromagnetic systems. We find that the two-magnon noise can signal the precipitation of a Bose-Einstein condensation (BEC).

Model.—In this Letter, we focus, for simplicity, on axially symmetric magnetic insulating films with approximate U(1) symmetry and a strong collinear order. In such systems, the net spin parallel to the magnetic symmetry axis is (approximately) conserved. The spin-wave dynamics can then be described in terms of transport of the conserved component of the spin density, and, moreover, we can introduce a well-defined magnon chemical potential [15–17]. In the setup we envision, illustrated in Fig. 2, a QI spin $\mathbf{S}_{\rm QI}$ is placed at a height d above a magnetic film and it is oriented along its anisotropy axis $\mathbf{n}$, with $\mathbf{z}\cdot\mathbf{n} = \cos\theta$. With a NV center in mind [1], we set $|\mathbf{S}_{\rm QI}| = 1$. The local spin density $\mathbf{s}(\mathbf{r})$ of the magnetic film generates a stray field $\mathbf{B}(\mathbf{r}_{\rm QI}) = \gamma \int d^2\mathbf{r}\mathcal{D}(\mathbf{r},\mathbf{r}_{\rm QI})\mathbf{s}(\mathbf{r})$ at the QI position $\mathbf{r}_{\rm QI} = (0,0,d)$, where γ is the gyromagnetic ratio of the film and $\mathcal{D}$ the tensorial magnetostatic Green's function [18,19]. Up to leading order in perturbation theory, the Zeeman coupling between the QI spin and the stray field induces QI transitions between the spin states $m_s = 0 \leftrightarrow \pm1$ at the resonance frequency $\omega_\pm$. We find the corresponding transition rate as [20]

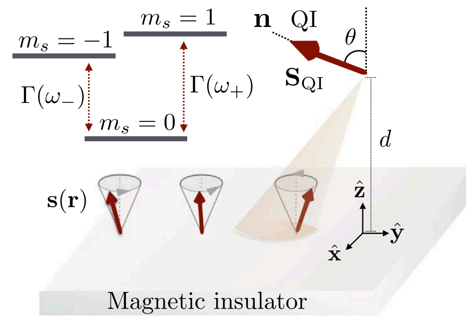

FIG. 2. Setup for QI relaxometry of a magnetic insulating system. The QI spin $\mathbf{S}_{\rm QI}$ is located at a height d above the magnetic film and oriented along its anisotropy axis $\mathbf{n}$, with $\mathbf{z}\cdot\mathbf{n} = \cos\theta$. The coordinate system has the xy plane placed on the magnetic film, with the origin aligned with the QI position. The interactions between the QI spin and the local spin density $\mathbf{s}(\mathbf{r})$ of the magnetic film induce QI transitions between the spin states $m_s = 0 \leftrightarrow \pm1$ with energy loss or gain of $\hbar\omega_\pm$ at the rate $\Gamma(\omega_\pm)$.

$$\Gamma(\omega_\pm) = f(\theta)\int_0^\infty dkk^3 e^{-2kd}[C_{xx}(k,\omega_\pm) + C_{zz}(k,\omega_\pm)], \quad (1)$$

with $f(\theta) = (\gamma\tilde{\gamma})^2(5-\cos 2\theta)/16\pi$, where $\tilde{\gamma}$ is the QI gyromagnetic ratio. Here, $C_{xx(zz)}(k,\omega)$ is the Fourier transform of the spin-spin correlator $C_{xx(zz)}(\mathbf{r}_i,\mathbf{r}_j;t) = \langle\{\hat{s}_{x(z)}(\mathbf{r}_i,t),\hat{s}_{x(z)}(\mathbf{r}_j,0)\}\rangle$, which describes magnetic noise transverse (longitudinal) to the magnetic symmetry axis $\mathbf{z}$, i.e., to the equilibrium orientation of the order parameter. Here, we have introduced the spin density operator $\hat{\mathbf{s}}$, $\langle\ldots\rangle$ stands for the equilibrium (thermal) average and $\{\ldots\}$ for the anticommutator. Invoking the Holstein-Primakoff transformation [21], i.e., $\hat{s}^+ = \hat{s}_x + i\hat{s}_y \propto \hat{a}^\dagger$ and $\hat{s}_z \propto \hat{a}^\dagger\hat{a}$, with $\hat{a}^\dagger$ ($\hat{a}$) being the magnon creation (annihilation) operator, one can see that the transverse and longitudinal noises emerge from, respectively, one- and two-magnon processes. In the following, we assume the QI frequency to lie sufficiently within the magnetic gap, such that only two-magnon processes contribute, i.e., $C_{xx}(k,\omega_\pm) \to 0$ [22].

Diffusive transport properties via two-magnon noise.—The longitudinal noise, C_{zz}, can be related to the imaginary part, χ''_{zz}, of the longitudinal spin susceptibility via the fluctuation-dissipation theorem [7], i.e., $C_{zz}(k,\omega) = \coth(\beta\hbar\omega/2)\chi''_{zz}(k,\omega)$, with $\beta = 1/k_B T$ and k_B being the Boltzmann constant. Thus, the two-magnon driven QI relaxation rate is fully determined by the longitudinal spin susceptibility of the magnetic system. The latter depends on the pertinent spin-transport regime, and it can be obtained by inverting the corresponding spin-transport equation.

As an experimentally relevant example, here, we consider a weakly interacting magnon system, whose spin density dynamics can be treated as diffusive at wavelengths larger than the magnon mean free path (mfp) $\ell_{\rm mfp}$, i.e.,

$$\partial_t s_z + \nabla \cdot \mathbf{j}_s = -\frac{1}{\tau_s} s_z. \tag{2}$$

Here, we have introduced the spin-relaxation time τ_s and the spin current $\mathbf{j}_s = -\sigma \nabla \mu$, where σ is the magnon spin conductivity, $\mu = \chi^{-1} s_z - \gamma H$ the chemical potential, χ the static uniform longitudinal susceptibility, and H an external magnetic field. Introducing the diffusion coefficient $D = \sigma/\chi$, the imaginary part of the dynamical longitudinal spin susceptibility can be written as [23]

$$\chi''_{zz}(k,\omega) = \frac{\chi \hbar^2 \omega D k^2}{(Dk^2 + 1/\tau_s)^2 + \omega^2}. \tag{3}$$

One might notice that, in Eq. (1), the filtering function $k^3 e^{-2kd}$, introduced by dipolar interactions, is peaked around the wave vector $k \sim 1/d$: contributions to Eq. (1) from smaller wave vectors are algebraically suppressed as they have limited phase space, while the ones at larger wave vectors are exponentially suppressed due to the self-averaging of short-wavelength fluctuations [8]. This allows us to approximate $\chi''_{zz}(k) \sim \chi''_{zz}(1/d)$ [24]. For $\beta\hbar\omega \ll 1$, the QI relaxation rate reads as

$$\Gamma(\omega) \sim f(\theta) \frac{\hbar \chi}{\beta D d^2} \frac{1}{[1 + (\frac{d}{\ell_s})^2]^2 + (\frac{\omega d^2}{D})^2}, \tag{4}$$

where we have introduced the spin-diffusion length $\ell_s = \sqrt{D\tau_s}$. Measuring the QI relaxation rate while varying the distance between the QI and the magnetic film should then unveil the region over which a diffusive description of transport holds, according to Eq. (4), as well as the wavelength at which it starts breaking down. Equation (4) shows that the relaxation rate increases with decreasing frequency, up to becoming constant, i.e., $\Gamma \sim (d + d^3/\ell_s^2)^{-2}$, for $\omega \ll D/d^2$. In this regime, one can detect the region where $d \sim \ell_s$ as the crossover region between $\Gamma \sim d^{-2}$ and $\Gamma \sim d^{-6}$, as depicted in Fig. 3. Within such a region, we find that measuring the QI relaxation rates, $\Gamma(d_1)$ and $\Gamma(d_2)$, at two different distances, d_1 and d_2, leads to an estimate for the spin diffusion length as

$$\ell_s^2 \sim \frac{d_1^3 \sqrt{\Gamma(d_1)/\Gamma(d_2)} - d_2^3}{d_2 - d_1 \sqrt{\Gamma(d_1)/\Gamma(d_2)}}. \tag{5}$$

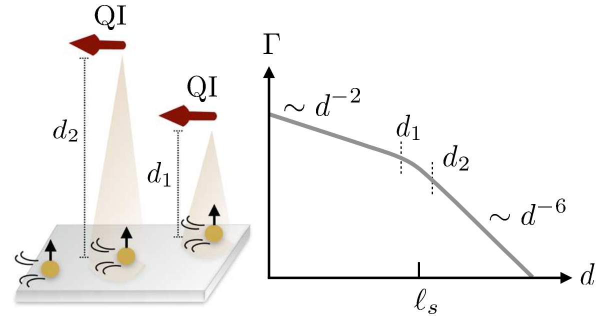

FIG. 3. Measurement of the spin diffusion length ℓ_s. By varying the distance d between the magnetic film and the quantum impurity, one can find a crossover region between two limiting behaviors of the QI relaxation rate Γ, i.e., $\Gamma \sim d^{-2}$ and $\Gamma \sim d^{-6}$. Within this region, measuring the relaxation rate at two different heights, d_1 and d_2, leads to an estimate for the spin diffusion length ℓ_s.

Since the spin-relaxation time τ_s and the susceptibility χ can be directly measured, one can use Eq. (5) to extract the magnon spin conductivity σ. Such a measurement, which could be performed by, e.g., embedding a NV center on a cantilever [25,26], would provide a direct probe of bulk spin-transport properties, not marred by interfacial effects that affect conventional spin-transport experiments [11]. The associated transport coefficients cannot be easily extracted from the one-magnon noise. Thus, our results suggest that, even when the spin-wave gap is lower than the maximum operating QI frequency, probing the subgap magnetic noise can provide a unique set of information.

Magnon BEC via two-magnon noise.—As an example of detection, via two-magnon noise, of a dynamical phase transition, we focus on magnon Bose-Einstein condensation and, therefore, investigate the dependence of the two-magnon noise on the magnon chemical potential. Our starting point is a general U(1)-symmetric Hamiltonian

$$\mathcal{H}_m = -J \sum_{\langle i \neq j \rangle} \hat{\mathbf{S}}_i \cdot \hat{\mathbf{S}}_j + \gamma \sum_i \hat{\mathbf{S}}_i \cdot \mathbf{H} + \frac{K}{2} \sum_i (\hat{S}_{z,i})^2, \tag{6}$$

where $\hat{\mathbf{S}}_i$ is the dimensionless on-site spin operator at the site $\mathbf{r}_i$ of a lattice, which, we take, for simplicity, to be square, $\mathbf{H} = H\mathbf{z}$ a uniform magnetic field, with $H > 0$, J the exchange stiffness, and K the constant governing the strength of the local anisotropy. First, we consider a ferromagnetic system with easy-plane anisotropy, i.e., J, $K > 0$. Introducing the Holstein-Primakoff transformation at leading order [21], we truncate the resulting Hamiltonian up to quadratic order and Fourier transform it. Equation (6) is diagonalized by a magnon mode with chemical potential μ and dispersion $\hbar\omega_{\mathbf{k}} = Ak^2 + \Delta_F$, where $A \sim JSa_0^2$ is the spin stiffness, a_0 the atomic spacing, and Δ_F the ferromagnetic gap. In the continuum limit, the QI spin couples to the coarse-grained spin density (in physical units).

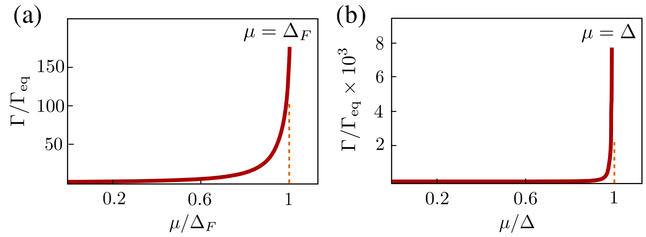

FIG. 4. QI relaxation rate as a function of the magnon chemical potential for a QI spin interacting with (a) a YIG film at $T = 100$ K, with $\omega = 1$ GHz; (b) a $MnFe_2$ film at $T = 10$ K, with $\omega = 10$ GHz. Each relaxation rate Γ is normalized by its respective value Γ_{eq} in equilibrium, i.e., for $\mu = 0$, while the magnon chemical potential is normalized by the spin-wave gap (Δ and Δ_F for the ferromagnetic and antiferromagnetic cases, respectively).

We approximate the dipolar kernel $\mathcal{D}(\mathbf{r} - \mathbf{r}_0)$ by a local coupling between the QI spin and the gradient of the longitudinal spin density, s_z, underneath it, and we set $\theta = 0$ [20,27].

As an example, we consider yttrium iron garnet (YIG), which is widely used in spintronic devices due to its long-range spin-transport properties. Taking $|\gamma| = |\tilde{\gamma}| = 2\mu_B/\hbar$, where μ_B is the Bohr magneton, and $A = 10^{-39}$ J m^2 [28], we plot, in Fig. 4(a), the two-magnon driven relaxation rate as a function of the chemical potential μ, having set $\Delta_F/\hbar = 10$ GHz, $\omega = 1$ GHz, $T = 100$ K, and $d = 100$ nm [20]. Figure 4(a) shows that, while increasing the magnon chemical potential, which could be achieved via, e.g., microwave pumping [9], the two-magnon noise increases logarithmically and reaches its saturation value in correspondence to the precipitation of Bose-Einstein condensation, i.e., $\mu = \Delta_F$. For $\hbar\omega \ll \Delta - \mu$, $\beta\Delta \ll 1$, and in proximity to the condensation point, i.e., $\mu \to \Delta$, the QI relaxation rate can be approximated as [20]

$$\Gamma \sim \frac{\hbar^3 (\gamma\tilde{\gamma})^2}{A^3 \beta^2} \ln\left(\frac{A}{d^2(\Delta_F - \mu)}\right). \tag{7}$$

In equilibrium (i.e., $\mu = 0$), $\Gamma^{-1} \sim 10$ ms, while at the onset of BEC, the QI relaxation time decreases up to $\Gamma^{-1} \sim 100\ \mu$s [29]. The latter is much shorter than the intrinsic relaxation time of, e.g., NV centers, which can reach seconds at $T \sim 100$ K [30], suggesting that the signal is detectable in practice.

Next, we consider an antiferromagnetic system with easy-axis anisotropy, whose energetics can be described by Eq. (6) setting $K, J \to -K, -J$, while keeping $K, J > 0$. Introducing the Holstein-Primakoff transformation up to leading order and, consequently, a Bogoliubov transformation (see, e.g., Ref. [31]), we can diagonalize the resulting Fourier transform of Eq. (6) in terms of two magnon eigenmodes, each one carrying spin angular momentum $\pm\hbar$, whose distribution functions are characterized by the dispersion $\hbar\omega_{\mathbf{k}} \mp \gamma H$ and chemical potential $\pm\mu$ [17]. Here, we have introduced $\hbar\omega_{\mathbf{k}} = \sqrt{\Delta^2 + (ck)^2}$, with $c \sim JSa_0$ being the spin-wave velocity and Δ the antiferromagnetic gap. The QI spin couples to the coarse-grained spin density (in physical units) of both sublattices. Focusing on the antiferromagnetic insulator $MnFe_2$, we take $c = 10^{-31}$ J m (having set $a_0 = 4$ Å) and $\Delta/\hbar = 1$ THz [31]. We set $d = 100$ nm, $T = 10$ K, $\omega = 10$ GHz, and $H = 0$. Figure 4(b) shows that the QI relaxation rate increases logarithmically with increasing chemical potential, in analogy with the ferromagnetic case [20]. Indeed, for $\omega \ll \Delta - \mu$, $\beta\Delta \ll 1$, and in proximity of the condensation point, i.e., $\mu \to \Delta$, the relaxation rate can be approximated as [20]

$$\Gamma \sim \frac{\hbar^3 (\gamma\tilde{\gamma})^2 \Delta^3}{c^6 \beta^2} \ln\left[\frac{A}{d^2(\Delta - \mu)}\right]. \tag{8}$$

In equilibrium (i.e., $\mu = 0$), $\Gamma^{-1} \sim 10$ ms, while at the onset of BEC, the QI relaxation time decreases up to $\Gamma^{-1} \sim 1\ \mu$s [29]. As could be expected, the QI relaxation rate decreases with increasing distance d (albeit only logarithmically), as shown by Eqs. (7) and (8).

Discussion.—Although the QI relaxometry of magnetic insulators has, so far, been primarily focused on the one-magnon noise [9], subgap magnetic fluctuations have been recently detected near a YIG film [32]. In this Letter, we relate the leading-order subgap magnetic noise to two-magnon Raman processes. We show that two-magnon driven QI relaxometry can be used as a direct probe of spin-wave bulk transport properties of magnetic insulators, which cannot be easily extracted from the one-magnon noise. With the growing interest in insulating systems with long-range spin-transport capabilities, we propose QI relaxometry as a direct probe of key quantities such as the spin-diffusion coefficient and spin-relaxation time, without a need to fabricate metal-insulator heterostructures. While we have, for simplicity, focused on the diffusive transport, our framework can also be applied to other transport regimes.

Our results suggest that magnon Bose-Einstein condensation can be detected via two-magnon noise in both ferromagnetic and antiferromagnetic systems. Our findings can be readily tested experimentally in ferromagnetic insulators, such as YIG, and, most importantly, they open up new prospects for detecting magnon condensation, induced by, e.g., thermal gradients [33], in antiferromagnetic insulators. With its combined capabilities, QI relaxometry of the two-magnon noise can also shed light on spin transport and dynamics in systems in which thermal spin waves coexist with a superfluid condensate of magnons [34].

In this work, we focused on magnetic insulators, where, due to the lack of charge noise, we can directly relate the QI relaxation rates to one- and two-magnon processes.

Our theory, however, can also be applied to conducting materials, in the regimes where the magnetostatic noise associated with spin-density fluctuations dominates over the electronic (Johnson-Nyquist) noise.

Future work should investigate the role of higher-order magnon processes. While generically, at lower temperatures, we may expect for such processes to give only small corrections, they might become important at the onset of a singularity, such as that triggered by the magnon Bose-Einstein condensation [cf. Eqs. (7) and (8)]. This may affect the fate of the logarithmic singularity derived here, at the onset of a dynamic phase transition.

The authors thank T. van der Sar and C. Du for insightful discussions and the International Institute of Physics in Natal, Brazil, where this work was initiated, for their generous hospitality. B. F. was supported by the Dutch Science Foundation (NWO) through a Rubicon grant and Y. T. by NSF under Grant No. DMR-1742928.

[1] M. W. Doherty, N. B. Manson, P. Delaney, F. Jelezko, J. Wrachtrup, and L. C. L. Hollenberg, Phys. Rep. **528**, 1 (2013).

[2] J. M. Taylor, P. Cappellaro, L. Childress, L. Jiang, D. Budker, P. R. Hemmer, A. Yacoby, R. Walsworth, and M. D. Lukin, Nat. Phys. **7**, 270 (2011).

[3] L. M. Pham, D. Le Sage, P. L. Stanwix, T. K. Yeung, D. Glenn, A. Trifonov, P. Cappellaro, P. R. Hemmer, M. D. Lukin, H. Park, A. Yacoby, and R. L. Walsworth, New J. Phys. **13**, 045021 (2011).

[4] S. Hong, M. S. Grinolds, L. M. Pham, D. Le Sage, L. Luan, R. L. Walsworth, and A. Yacoby, MRS Bull. **38**, 155 (2013).

[5] M. S. Grinolds, S. Hong, P. Maletinsky, L. Luan, M. D. Lukin, R. L. Walsworth, and A. Yacoby, Nat. Phys. **9**, 215 (2013).

[6] F. Casola, T. van der Sar, and A. Yacoby, Nat. Rev. Mater. **3**, 17088 (2018).

[7] R. Kubo, Rep. Prog. Phys. **29**, 255 (1966).

[8] K. Agarwal, R. Schmidt, B. Halperin, V. Oganesyan, G. Zarand, M. D. Lukin, and E. Demler, Phys. Rev. B **95**, 155107 (2017).

[9] C. Du, T. van der Sar, T. X. Zhou, P. Upadhyaya, F. Casola, H. Zhang, M. C. Onbasli, C. A. Ross, R. L. Walsworth, Y. Tserkovnyak, and A. Yacoby, Science **357**, 195 (2017).

[10] L. J. Cornelissen, J. Liu, R. A. Duine, J. Ben Youssef, and B. J. van Wees, Nat. Phys. **11**, 1022 (2015).

[11] L. J. Cornelissen, K. J. H. Peters, G. E. W. Bauer, R. A. Duine, and B. J. van Wees, Phys. Rev. B **94**, 014412 (2016).

[12] A. V. Chumak, V. I. Vasyuchka, A. A. Serga, and B. Hillebrands, Nat. Phys. **11**, 453 (2015).

[13] T. van der Sar, F. Casola, R. Walsworth, and A. Yacoby, Nat. Commun. **6**, 7886 (2015).

[14] V. Baltz, A. Manchon, M. Tsoi, T. Moriyama, T. Ono, and Y. Tserkovnyak, Rev. Mod. Phys. **90**, 015005 (2018).

[15] B. I. Halperin and P. C. Hohenberg, Phys. Rev. **188**, 898 (1969).

[16] S. A. Bender, R. A. Duine, and Y. Tserkovnyak, Phys. Rev. Lett. **108**, 246601 (2012).

[17] B. Flebus *et al.* (to be published).

[18] Here, $\mathcal{D}_{\alpha\beta}(\vec{r}, \vec{r}_{\mathrm{QI}}) = -(\partial^2/\partial\vec{r}_\alpha \partial\vec{r}_{\mathrm{QI},\beta})|\vec{r} - \vec{r}_{\mathrm{QI}}|^{-1}$ with $\alpha, \beta = x, y, z$ [19].

[19] K. Y. Guslienko and A. N. Slavin, J. Magn. Magn. Mater. **323**, 2418 (2011).

[20] See Supplemental Material at http://link.aps.org/supplemental/10.1103/PhysRevLett.121.187204, where we derived the relaxation rate of a QI spin interacting with the spin density of a $U(1)$-symmetric magnetic insulating film, Eq. (1), and calculated the two-magnon driven QI relaxation rate at the onset of magnon Bose-Einstein condensation, Eqs. (7) and (8).

[21] T. Holstein and H. Primakoff, Phys. Rev. **58**, 1098 (1940).

[22] Relaxation Γ_s of spin dynamics gives rise to a broadening in the magnetic-resonance absorption spectrum. The single-magnon noise would decay rapidly within the subgap region, essentially vanishing at frequencies $\omega < \Delta - \Gamma_s$. This regime can be easily achieved with, e.g., an NV center, whose zero-field splitting is $\omega = 2\pi \times 2.87$ GHz. An external magnetic field can shift one of the transitions to even lower frequencies, if needed.

[23] Note that, while the diffusion coefficient D and other parameters relating to the propagation and relaxation of thermal magnons generally depend on the magnon gap (which in turn can depend on various details, such as the applied field, crystalline anisotropies, elastic strain, etc.), this dependence can be expected to be weak at temperatures much higher than the gap.

[24] Without resorting to approximations, the QI relaxation rate associated with Eq. (3) can be found as $\Gamma(\omega) = f(\theta)\coth(\beta\hbar\omega/2)(\chi\hbar^2/4\sqrt{\pi}d^4)\sum_{\alpha=\pm}\alpha G^{3,1}_{0,0}(0,2,5/2(d^2/\ell_s^2) + (\alpha i\omega d^2/D))$, where $G^{m,n}_{p,q}(a_1,\ldots,a_p b_1,\ldots,b_q z)$ is the Meijer G function.

[25] T. X. Zhou, R. J. Stohr, and A. Yacoby, Appl. Phys. Lett. **111**, 163106 (2017).

[26] L. Rondin, J.-P. Tetienne, P. Spinicelli, C. Dal Savio, K. Karrai, G. Dantelle, A. Thiaville, S. Rohart, J.-F. Roch, and V. Jacques, Appl. Phys. Lett. **100**, 153118 (2012).

[27] Note that a different choice for the anisotropy axis orientation θ would only affect the overall multiplication factor.

[28] B. A. Kalinikos and A. N. Slavin, J. Phys. C **19**, 7013 (1986).

[29] These values refer to our numerical solution for the QI relaxation rate [20].

[30] N. Bar-Gill, L. M. Pham, A. Jarmola, D. Budker, and R. L. Walsworth, Nat. Commun. **4**, 1743 (2013).

[31] S. M. Rezende, R. L. Rodriguez-Suarez, and A. Azevedo, Phys. Rev. B **93**, 054412 (2016).

[32] C. Du (private communication).

[33] Y. Tserkovnyak, S. A. Bender, R. A. Duine, and B. Flebus, Phys. Rev. B **93**, 100402 (2016).

[34] B. Flebus, S. A. Bender, Y. Tserkovnyak, and R. A. Duine, Phys. Rev. Lett. **116**, 117201 (2016).

Supplemental Material: Quantum-Impurity Relaxometry of Magnetic Dynamics

B. Flebus and Y. Tserkovnyak
Department of Physics and Astronomy, University of California, Los Angeles, California 90095, USA

In this supplemental material, we derive the relaxation rate of a quantum-impurity spin interacting with the spin density of a U(1)-symmetric magnetic insulating film. Moreover, we provide a derivation of the two-magnon driven QI relaxation rate at the onset of magnon Bose-Einstein condensation, both for a ferromagnetic and an antiferromagnetic system.

Quantum-impurity relaxation rate. We consider the Zeeman coupling between a QI quantum spin $\hat{\mathbf{S}}_{\rm qi}$, with $|\hat{\mathbf{S}}_{\rm qi}|$=1, and the stray field operator $\hat{\mathbf{B}}$. By introducing the operator $\hat{\mathbf{B}}_{\rm qi}=\mathcal{R}_x(\theta)\hat{\mathbf{B}}$, where $\mathcal{R}_x(\theta)$ is the rotation matrix such that $\mathcal{R}_x(\theta)\mathbf{n}=\mathbf{z}$, we can write

$$\mathcal{H}_{\rm int}=-\frac{\tilde{\gamma}}{2}\left(\hat{S}^+_{\rm qi}\hat{B}^-_{\rm qi}+\hat{S}_{{\rm qi},z}\hat{B}_{{\rm qi},z}+{\rm H.c}\right)\,, \tag{S1}$$

where we have introduced $\hat{B}^{\pm}_{\rm qi}=\hat{B}_{{\rm qi},x}\pm i\hat{B}_{{\rm qi},y}$ and $\hat{S}^{\pm}_{\rm qi}=\hat{S}_{{\rm qi},x}\pm i\hat{S}_{{\rm qi},y}$. The QI relaxation rate at frequency ω can be found, to leading order in perturbation theory, as

$$\Gamma(\omega)=\frac{\tilde{\gamma}^2}{2}\int dt\, e^{-i\omega t}\langle\{\hat{B}^+_{\rm qi}(t),\hat{B}^-_{\rm qi}(0)\}\rangle. \tag{S2}$$

For a QI spin at a height d above the magnetic system, the field operator can be written explicitely as

$$\hat{B}^-_{\rm qi}=\gamma\int d^2\mathbf{r}\left[a_{\theta,d,\mathbf{r}}\hat{s}^+(\mathbf{r})+b_{\theta,d,\mathbf{r}}\hat{s}^-(\mathbf{r})+c_{\theta,d,\mathbf{r}}\hat{s}_z(\mathbf{r})\right]\,, \tag{S3}$$

with

$$\begin{aligned}a_{\theta,d,\mathbf{r}}=&\frac{1}{2}\big[\mathcal{D}_{xx}(\mathbf{r},d)+i(1-\cos\theta)\mathcal{D}_{xy}(\mathbf{r},d)\\&+\mathcal{D}_{yy}(\mathbf{r},d)\cos\theta+i\mathcal{D}_{xz}(\mathbf{r},d)\sin\theta-\mathcal{D}_{yz}(\mathbf{r},d)\sin\theta\big]\,,\\b_{\theta,d,\mathbf{r}}=&\frac{1}{2}\big[\mathcal{D}_{xx}(\mathbf{r},d)-i(1+\cos\theta)\mathcal{D}_{xy}(\mathbf{r},d)\\&-\mathcal{D}_{yy}(\mathbf{r},d)\cos\theta+i\mathcal{D}_{xz}(\mathbf{r},d)\sin\theta+\mathcal{D}_{yz}(\mathbf{r},d)\sin\theta\big]\,,\\c_{\theta,d,\mathbf{r}}=&\mathcal{D}_{xz}(\mathbf{r},d)-i\mathcal{D}_{yz}(\mathbf{r},d)\cos\theta+i\mathcal{D}_{zz}(\mathbf{r},d)\sin\theta\,.\end{aligned} \tag{S4}$$

In a U(1)-symmetric system, the transverse spin response is completely decoupled from the longitudinal spin response [S1]. Thus, we can set $\langle\hat{s}^{\pm}(\mathbf{r}',t)\hat{s}_z(\mathbf{r},0)\rangle=0$. Moreover, U(1) symmetry requires $\langle\hat{s}_x(\mathbf{r}',t)\hat{s}_x(\mathbf{r},0)\rangle=\langle\hat{s}_y(\mathbf{r}',t)\hat{s}_y(\mathbf{r},0)\rangle$. We can then rewrite Eq. (S2) as [S2]

$$\begin{aligned}\Gamma(\omega)=&\frac{(\gamma\tilde{\gamma})^2}{2}\int\frac{d^2\mathbf{k}}{(2\pi)^2}\Big[|a_{\theta,d,\mathbf{k}}|^2C_{+-}(\mathbf{k},\omega)\\&+a^*_{\theta,d,\mathbf{k}}b_{\theta,d,\mathbf{k}}C_{++}(\mathbf{k},\omega)+a_{\theta,d,\mathbf{k}}b^*_{\theta,d,\mathbf{k}}C_{--}(\mathbf{k},\omega)\\&+|b_{\theta,d,\mathbf{k}}|^2C_{-+}(\mathbf{k},\omega)+|c_{\theta,d,\mathbf{k}}|^2C_{zz}(\mathbf{k},\omega)\Big]\,,\end{aligned} \tag{S5}$$

where $C_{\alpha\beta}(\mathbf{k},\omega)$ is the Fourier transform of the spin-spin correlator $C_{\alpha\beta}(\mathbf{r},\mathbf{r}';t)=\langle\{\hat{s}^{\alpha}(\mathbf{r}',t),\hat{s}^{\beta}(\mathbf{r},0)\}\rangle$, with $\alpha,\beta=\pm$ and where translational symmetry dictates $C_{\alpha\beta}(\mathbf{r},\mathbf{r}';\omega)=C_{\alpha\beta}(|\mathbf{r}-\mathbf{r}'|,\omega)$. Rewriting the Fourier transform of the magnetostatic Green's function tensor $\mathcal{D}(\mathbf{r},\mathbf{r}')$ as

$$\mathcal{D}(\mathbf{k})=-e^{-dk}k\begin{pmatrix}\cos^2\phi_{\mathbf{k}} & \sin(2\phi_{\mathbf{k}})/2 & i\cos\phi_{\mathbf{k}}\\ \sin(2\phi_{\mathbf{k}})/2 & \sin^2\phi_{\mathbf{k}} & i\sin\phi_{\mathbf{k}}\\ i\cos\phi_{\mathbf{k}} & i\sin\phi_{\mathbf{k}} & -1\end{pmatrix}\,, \tag{S6}$$

and $C_{\alpha\beta}(\mathbf{k},\omega)=C_{\alpha\beta}(k,\omega)$ (with $k=|\mathbf{k}|$), Eq. (S5) becomes

$$\Gamma(\omega)=f(\theta)\int_0^{\infty}dk\,k^3e^{-2kd}\left[C_{xx}(k,\omega)+C_{zz}(k,\omega)\right]\,, \tag{S7}$$

with $f(\theta)=(\gamma\tilde{\gamma})^2(5-\cos2\theta)/16\pi$, which corresponds to Eq. (1) of the main text.

Two-magnon noise at BEC. In the regime where the magnetic noise is dominated by two-magnon processes, the stray field at the QI position $\mathbf{r}_{\rm qi}$ can be written as $\mathbf{B}_{\rm qi}(\mathbf{r}_{\rm qi})=\gamma\int d^2\mathbf{r}\;\;\mathcal{R}_x(\theta)\sum_{i=1}^3\mathcal{D}_{i3}(\mathbf{r}-\mathbf{r}_{\rm qi})s_z(\mathbf{r})$. Focusing on excitations at wavelengths much longer than the distance d between the quantum impurity and the magnetic film, we can perform a gradient expansion of the z-component of the spin density, i.e., $s_z(x,y)\simeq s_z(0,0)+\partial_xs_z(0,0)x+\partial_ys_z(0,0)y$. The relevant magnetostatic Green's functions can be rewritten in polar coordinates as

$$\mathcal{D}_{13}(\rho,\phi,d)=-\frac{3d\rho\cos\phi}{(d^2+\rho^2)^{\frac{5}{2}}}\,,\quad\mathcal{D}_{33}(\rho,d)=\frac{2d^2-\rho^2}{(d^2+\rho^2)^{\frac{5}{2}}}\,, \tag{S8}$$

and $\mathcal{D}_{23}(\rho,\phi,d)=\mathcal{D}_{13}(\rho,\phi,d)$ with $\cos\phi\to\sin\phi$. Performing an integration over the coordinates ϕ and ρ, we find the circularly-polarized stray field operator as

$$\hat{B}^-=2\pi\gamma\left[i\partial_y\hat{s}_z(0,0)\cos\theta-\partial_x\hat{s}_z(0,0)\right]\,. \tag{S9}$$

By setting $\theta=0$, the relaxation rate associated to Eq. (S9) simplifies to

$$\Gamma(\omega)=\pi(\gamma\tilde{\gamma})^2\int_0^{1/d}dk\,k^3C_{zz}(k,\omega)\,. \tag{S10}$$

For a ferromagnetic system described by the Hamiltonian (6), the longitudinal spin-spin correlation function can be found as

$$C_{zz}(\mathbf{q},\omega) = \frac{\hbar^2}{4\pi}\coth\left(\frac{\beta\hbar\omega}{2}\right)\int d^2\mathbf{k}\,\delta(\omega_{\mathbf{k}}-\omega_{\mathbf{k+q}}+\omega) \times \{n_B[\beta(\hbar\omega_{\mathbf{k}}-\mu)] - n_B[\beta(\hbar\omega_{\mathbf{k+q}}-\mu)]\}\,, \tag{S11}$$

where $n_B(x) = (e^x-1)^{-1}$ is the Bose-Einstein distribution function and $\hbar\omega_{\mathbf{k}} = Ak^2 + \Delta_F$ the magnon dispersion. By plugging Eq. (S11) into Eq. (S10), for $\hbar\omega, \Delta_F \ll \beta^{-1}$, we find

$$\Gamma(\omega) = \frac{\pi\hbar^3(\gamma\tilde{\gamma})^2}{4A^3\beta^2}\int_0^{\epsilon_d} d\epsilon \frac{\epsilon}{(\epsilon+\Delta_F-\mu+\hbar\omega)(\epsilon+\Delta_F-\mu)}\,, \tag{S12}$$

where $\epsilon_d = A/d^2$. Carrying out explicity the integration, Eq. (S12) becomes

$$\Gamma(\omega) = \frac{\pi\hbar^3(\gamma\tilde{\gamma})^2}{4A^3\beta^2}\left[\frac{\Delta_F-\mu}{\hbar\omega}\ln\left(\frac{\Delta_F-\mu}{\epsilon_d+\Delta_F-\mu}\right) - \frac{\Delta_F-\mu+\hbar\omega}{\hbar\omega}\ln\left(\frac{\Delta_F-\mu+\hbar\omega}{\epsilon_d+\Delta_F-\mu+\hbar\omega}\right)\right]. \tag{S13}$$

We take $\omega = 1$ GHz, $T = 100$ K and $d = 100$ nm. With YIG in mind, we set $\Delta_F/\hbar = 10$ GHz and $A = 10^{-39}$ J · m^2 [25], which leads to $\epsilon_d/\hbar \approx 1$ GHz. In Fig. 4(a) of the main text, we plot Eq. (S13) as function of the magnon chemical potential μ for these parameters. Approaching the condensation point, i.e., $\mu \to \Delta$, for $\omega \ll \Delta - \mu$, Eq. (S13) can be approximated as

$$\Gamma \sim \frac{\hbar^3(\gamma\tilde{\gamma})^2}{A^3\beta^2}\ln\frac{A}{d^2\,(\Delta_F-\mu)}\,, \tag{S14}$$

which corresponds to Eq. (7) of the main text.

For an antiferromagnetic system described by Eq. (6), the longitudinal spin-spin correlation function, for $\hbar\omega \ll \Delta$, can be derived as

$$C_{zz}(\omega,\mathbf{q}) = \coth\left(\frac{\beta\hbar\omega}{2}\right)\frac{\hbar^2}{4\pi}\int d^2\mathbf{k} \times \left[\delta(\omega_{\mathbf{k}}-\omega_{\mathbf{k+q}}+\omega)u_{\mathbf{k}}^2 + \delta(\omega_{\mathbf{k}}-\omega_{\mathbf{k+q}}-\omega)v_{\mathbf{k}}^2\right] \times \{n_B[\beta(\hbar\omega_{\mathbf{k}}-\mu)] - n_B[\beta(\hbar\omega_{\mathbf{k+q}}-\mu)] + n_B[\beta(\hbar\omega_{\mathbf{k}}+\mu)] - n_B[\beta(\hbar\omega_{\mathbf{k+q}}+\mu)]\}, \tag{S15}$$

with $\hbar\omega_{\mathbf{k}} = \sqrt{\Delta^2+(ck)^2}$, $\mu \to \mu - H$, and where we have introduced the Bogoliubov coefficients

$$u_{\mathbf{k}} = \sqrt{\frac{\omega_{ZB}+\omega_{\mathbf{k}}}{2\omega_{\mathbf{k}}}},\quad v_{\mathbf{k}} = \sqrt{\frac{\omega_{ZB}-\omega_{\mathbf{k}}}{2\omega_{\mathbf{k}}}}\,, \tag{S16}$$

with $\omega_{ZB} = \sqrt{2(c/a_0)^2+\Delta^2}$. An external bias, e.g., a RF circularly-polarized field, can trigger the condensation of one of the two antiferromagnetic magnon modes. Here, we focus on the mode carrying spin angular momentum $\hbar$, whose condensation occurs for $\Delta = \mu$. For $\Delta \ll \beta^{-1}$, we can rewrite the relaxation rate as

$$\Gamma(\omega) = \frac{\pi\hbar^3(\gamma\tilde{\gamma})^2}{2c^6\beta^2}\left[\int_{\Delta}^{\tilde{\epsilon}_d} d\epsilon\,\frac{\epsilon^2(\epsilon^2-\Delta^2)}{(\epsilon+\hbar\omega-\mu)(\epsilon-\mu)}\left(\frac{\omega_{ZB}}{\epsilon}+1\right) + \int_{\Delta+\hbar\omega}^{\tilde{\epsilon}_d} d\epsilon\,\frac{\epsilon^2(\epsilon^2-\Delta^2)}{(\epsilon-\hbar\omega-\mu)(\epsilon-\mu)}\left(1-\frac{\omega_{ZB}}{\epsilon}\right)\right] + (\mu\to-\mu)\,. \tag{S17}$$

with $\tilde{\epsilon}_d = \sqrt{(c/d)^2+\Delta^2}$. We set $d = 100$ nm, $T = 10$ K and $\omega = 10$ GHz. Considering $MnFe_2$, we take $c = 10^{-31}$ J · m, $a_0 \approx 4$ Å, $\Delta/\hbar = 1$ THz [29] and, for simplicity, we set $H = 0$. In Fig. 4(b) of the main text, we plot Eq. (S17) for these parameters.

When the system approaches the condensation point, i.e., $\mu \to \Delta$, for $\hbar\omega \ll \Delta - \mu$, the integrand (S17) displays a singularity at the bottom of the magnon dispersion, where the magnon dispersion is quadratic. Hence, one might expect a divergence analogous to Eq. (S14). Indeed, we find that, for $\mu \to \Delta$, with $\omega \ll \Delta - \mu$, Eq. (S17) can be approximated as

$$\Gamma \sim \frac{\hbar^3(\gamma\tilde{\gamma})^2\Delta^3}{c^6\beta^2}\ln\frac{A}{d^2\,(\Delta-\mu)}\,, \tag{S18}$$

which corresponds to Eq. (8) of the main text.

[S1] G. F. Giuliani, and G. Vignale, *Quantum Theory of the Electron Liquid* (Cambridge University Press, Cambridge, 2005).

[S2] In nonmagnetic (i.e., time-reversal invariant) systems with U(1) symmetry, $C_{++} = C_{--} = 0$ [S1]. For an isotropic magnetic film (which we will assume), while these correlators are present in principle, their contributions to the QI relaxation rate cancel out upon the angular integration in the momentum space.